Journal of Brilliant Engineering 3 (2025) 41040
Brilliant Engineering
journal home: www.acapublishing.com/journals/4/ben
Research Article

Design, Parametric Analysis, and Experimental Validation of a Screen-Printed Flexible Band-Stop Frequency Selective Surface

Hakan Kiziltas*,[1], Gokhan Ozturk[2]
[1,2]Department of Electrical-Electronics Engineering, Atatürk University, Erzurum, Türkiye

Keywords

Frequency selective Surface (FSS), Metamaterial, Reflective band-stop filter, Conductive polymer coating, Electromagnetic shielding.

Abstract

This study presents the design, simulation, fabrication, and experimental validation of a ring-shaped frequency-selective surface (FSS) applied onto textile using conductive polyurethane-based paint. The FSS was modeled in CST Studio Suite and optimized to achieve strong electromagnetic attenuation through a reflective band-stop mechanism in the 2–8 GHz frequency range. Simulation results revealed a resonance dip in the transmission coefficient (S_{21}) at approximately 6.00 GHz, with a suppression level of −28 dB and a −10 dB bandwidth of approximately 1.7 GHz. The corresponding reflection coefficient (S_{11}) was measured at approximately −3 dB, indicating dominant reflection and partial absorption (~50%), consistent with reflective band-stop filter behavior. A prototype was fabricated via screen printing the conductive paint onto a 150 mm × 150 mm textile substrate. Experimental measurements using a vector network analyzer (VNA) confirmed the band-stop performance and showed good agreement with the simulations. The proposed hybrid structure effectively integrates the electromagnetic functionality of metamaterials with the flexibility of textiles, making it suitable for applications such as electromagnetic shielding, stealth technology, and wearable electronics. The fabrication technique offers a scalable, low-cost solution for large-area, flexible, and conformal electromagnetic surfaces.

1. Introduction

Frequency-Selective Surfaces (FSSs) are periodic two-dimensional structures capable of filtering, reflecting, or absorbing electromagnetic (EM) waves, depending on the frequency. Typically composed of regularly arranged metallic or conductive patterns printed on dielectric substrates, FSSs function as spatial filters and have found applications in radomes, wireless communications, stealth systems, and electromagnetic interference (EMI) shielding. Their frequency response is largely determined by the geometry, size, and periodicity of the unit cells, as well as the electrical and dielectric properties of the substrate material. By carefully adjusting these parameters, engineers can design FSSs with sharp resonance characteristics, wideband performance, and insensitivity to variations in polarization or incident angle [1–3].

Despite their versatility, conventional FSSs are generally fabricated on rigid substrates using photolithography or printed circuit board (PCB) techniques. While such methods yield high precision and conductivity, they are often expensive, inflexible, and unsuitable for applications requiring stretchable or conformable designs. As modern electronics evolve toward flexible, wearable, and embedded systems, there is a growing demand for alternative FSS configurations that can be integrated with lightweight, deformable, and low-cost substrates such as textiles, polymers, or paper [4–6].

In recent years, significant attention has been devoted to integrating FSSs into textile platforms. Textile-based FSSs are promising for emerging applications, including wearable EM shielding, health-monitoring garments, reconfigurable antennas, and energy-harvesting clothing. However, achieving robust EM performance on soft, porous, and mechanically dynamic textile surfaces remains a significant challenge due to issues such as poor conductivity uniformity, material incompatibility, and structural deformation during use [7–11].

To overcome these barriers, various printing and deposition techniques have been investigated for transferring conductive patterns onto textiles. Among them, screen printing stands out as a scalable, low-cost, and fabric-compatible method that allows for precise patterning using conductive inks or paints. Polymer-based conductive coatings, particularly those using carbon- or metal-filled polyurethane (PU), are of special interest for their flexibility, environmental resistance, and good adhesion to textile surfaces [12–15].

Simultaneously, the rise of metamaterials has revolutionized EM device design. These engineered materials exhibit unconventional electromagnetic responses—such as negative permittivity, negative permeability, and zero-index behavior—not found in natural media [16,17]. When applied to FSSs, metamaterial concepts enable enhanced features, including strong absorption, tunability, and compactness. Metamaterial absorbers can achieve near-unity absorption by suppressing both reflection and transmission, which is advantageous for stealth, EM wave manipulation, and compact device integration [18–20].

However, most metamaterial absorbers rely on rigid substrates and cleanroom fabrication, which limits their usability in wearable or large-area, flexible systems. Moreover, many reported designs remain confined to simulations, with limited experimental validation due to fabrication difficulties [21]. Recent advances have focused on flexible and textile-based metamaterial absorbers, offering enhanced conformability and multi-band performance [22, 24].

*Corresponding Author: h.kiziltas@atauni.edu.tr
Received 23 Jul 2025; Revised 25 Jul 2025; Accepted 25 Jul 2025
https://doi.org/10.36937/ben.2025.41040
2687-5195 /© 2022 The Authors, Published by ACA Publishing; a trademark of ACADEMY Ltd. All rights reserved.

This study addresses these limitations by presenting a metamaterial-inspired, ring-shaped FSS structure screen-printed on a textile substrate using carbon-filled polyurethane-based conductive paint. The ring geometry was chosen due to its well-documented resonance properties, polarization independence, and planar compatibility. Compared to conventional FSS geometries such as cross-dipoles or Jerusalem crosses, the ring-shaped configuration offers polarization insensitivity and supports higher angular stability. Its continuous, symmetrical design ensures uniform current distribution and effective absorption over a broader bandwidth, making it more suitable for textile integration. The design was numerically optimized using CST Studio Suite to operate within the S-band (2–8 GHz), with a clear resonance observed at approximately 6.0 GHz. Simulations revealed strong electromagnetic attenuation, with a peak transmission suppression of approximately −28 dB and a −10 dB bandwidth of around 1.7 GHz, indicating effective band-stop and partial absorption behavior.

For fabrication, the conductive pattern was transferred onto a 150 mm × 150 mm textile substrate via screen printing, followed by thermal curing to enhance pattern stability and electrical performance. Experimental measurements using a vector network analyzer (VNA) validated the band-stop behavior and showed good agreement with the simulation results, with a deviation of only ±0.05 GHz from the simulated resonance frequency.

This work demonstrates the feasibility of developing high-performance, flexible, and low-cost FSS absorbers on textile platforms by combining metamaterial principles, carbon-filled PU inks, and scalable printing processes. The proposed structure retains its electromagnetic functionality under planar testing and is expected to be resilient under mechanical deformation, making it promising for wearable shielding, stealth garments, and other conformal EM applications.

This study also introduces several distinctive contributions compared to existing screen-printed textile FSS implementations.

First, the use of a custom-formulated, carbon-filled polyurethane-based conductive ink provides superior flexibility, wash resistance, and adhesion on porous textile substrates, which are often difficult to achieve simultaneously with traditional metallic inks.

Second, the ring-shaped resonator geometry, known for its polarization-insensitive and narrow-band properties, is here specifically optimized for textile-based substrates, ensuring high electromagnetic performance without compromising mechanical conformity.

Finally, the implementation of a screen-printing technique over a relatively large textile area (150 mm × 150 mm) demonstrates the scalability and practicality of the proposed method, validated through both simulation and experimental results. These combined features distinguish this work in terms of materials engineering, unit-cell design, and fabrication compatibility with flexible, wearable electromagnetic systems.

2. Materials and Methods

2.1. Materials

In this study, a woven polyester fabric measuring 150 mm × 150 mm was selected as the substrate due to its flexibility, durability, and compatibility with printing processes. The conductive material used to form the frequency-selective surface (FSS) patterns was a custom-formulated polyurethane (PU)-based ink filled with carbon black. The conductive ink formulation consisted of 85 wt.% PU resin and 15 wt.% carbon black, offering an optimal balance between electrical conductivity, mechanical flexibility, and adhesion to textile surfaces. This composition was optimized through preliminary trials: higher carbon loadings led to brittleness and clogging during printing, whereas lower carbon content resulted in poor conductivity.
The ink viscosity was adjusted using a small amount of butyl acetate solvent to ensure compatibility with the screen-printing process. The average surface roughness of the polyester textile was not measured quantitatively; however, the woven fabric exhibited a low-pile, tightly knit texture with minimal porosity, ensuring uniform ink deposition.

2.2. CST-Based unit cell design

The FSS structure was modeled using CST Studio Suite 2023, employing a full-wave frequency-domain electromagnetic solver. The fundamental dimensions and parameters used in the design of the ring-shaped FSS are as follows: The unit cell periodicity was set to x = y = 14 mm. The thickness of the dielectric layer was h = 0.5 mm, while the conductive surface thickness was c = 0.15 mm. The outer radius of the conductive surface was designed as r = 5.47 mm, and the width of the conductive ring was d = 0.5 mm.

The simulation domain was defined using periodic boundary conditions along the x- and y-axes, with open (add space) boundaries along the z-axis. Floquet ports were used to simulate normal wave incidence, and the frequency sweep was performed between 2 and 8 GHz. Mesh refinement was performed using adaptive passes to ensure numerical convergence. The final CST model is shown in Figure 1.

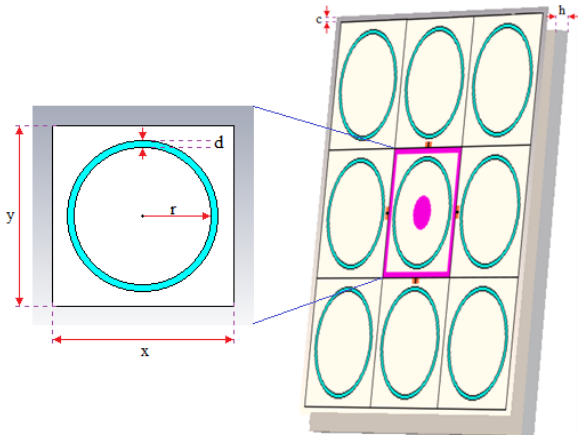

Figure 1. CST model of the ring-shaped FSS unit cell used in this study

In the CST simulations, the dielectric constant (ε_r) and loss tangent (tanδ) of the polyester fabric were assumed as 1.9 and 0.02, respectively, based on literature data for woven polyester substrates. The cured PU-based conductive ink was assigned a bulk electrical conductivity of approximately 2.1×10^3 S/m, measured using a four-point probe technique on a flat test sample. These values were used to ensure accurate modeling of the electromagnetic response and were validated through close agreement between simulation and experimental results.

In the simulation model, periodic boundary conditions were applied in the x and y directions using PEC and PMC walls, respectively. Open boundary conditions were applied along the z-direction. The convergence criterion for the frequency domain solver was set to a maximum delta S of 0.01 to ensure simulation accuracy.

A tetrahedral mesh type was used with a minimum mesh size of 0.2 mm, and full-wave convergence was ensured through 5 adaptive passes with a convergence threshold of 0.01.

2.3. Fabrication process

The designed FSS pattern was transferred onto the textile using a screen-printing technique. A stainless-steel stencil with a mesh density of 100 mesh/inch was prepared, and the conductive ink was applied using a manual squeegee. Thermal curing was performed at 120 °C for 15 minutes to stabilize the printed structure, ensuring ink fixation, pattern stability, and electrical continuity. To ensure consistent unit cell alignment, a pre-designed screen frame with registration marks was used, and the textile substrate was secured in place using masking tape to prevent displacement during printing. The resulting prototype consisted of a 5 × 5 array of ring-shaped unit cells printed over a 150 mm × 150 mm area. A representative photo of the printing process is shown in Figure 2.

Figure 2. Photograph of the screen-printing process used to fabricate the FSS on a textile substrate

After curing, the thickness of the printed conductive layer was measured using a digital micrometer and was found to be approximately 0.15 mm. This value is consistent with the ‘c’ parameter used in the CST simulation, confirming the fabrication–simulation match in terms of structural dimensions.

2.4. Experimental setup and characterization

To validate the simulation results, the fabricated FSS sample was tested using a Rohde & Schwarz ZNB20 vector network analyzer (VNA) in a standard two-port S_{11} reflection measurement setup. The measurements were performed in an anechoic environment using two standard horn antennas (WR-187, 2–8 GHz), positioned 40 cm apart with the sample placed at the midpoint. Calibration was performed using an open configuration without the sample.

3. Results and Discussion

This section presents both the simulation and experimental results of the proposed ring-shaped frequency-selective surface (FSS), designed as a band-stop filter in the 2–8 GHz range. The electromagnetic behavior was first analyzed using CST Studio simulations and then verified through experimental measurements using a vector network analyzer (VNA). The agreement between the numerical and experimental S-parameter responses validates the accuracy of the design and fabrication method." (Use "S-parameter" to include both S_{11} and S_{21}, which were measured.

In addition to evaluating the baseline structure, a comprehensive parametric study was conducted to investigate how key geometrical parameters affect the filter performance. Specifically, the effects of:

x: unit cell periodicity (spacing between resonators),

r: outer radius of the ring resonator, and

d: ring width (difference between outer and inner radius)

on the resonance frequency, bandwidth, and absorption level were systematically examined. Each parameter was varied individually while keeping the others constant to isolate its impact. The results of these parametric analyses are presented in the following subsections.

3.1. Effect of unit cell periodicity (x) on the S_{21} response

The unit cell periodicity (x) defines the center-to-center distance between adjacent ring-shaped resonators in the frequency-selective surface (FSS) array. In this study, x was systematically varied between 10 mm and 18 mm in 2 mm increments, while keeping all other parameters constant (r = 5.47 mm, and d = 0.5 mm).

As shown in Figure 3, increasing x resulted in a slight upward shift in the resonance frequency, moving from 5.89 GHz at x = 10 mm to 6.12 GHz at x = 18 mm. Additionally, the −10 dB bandwidth narrowed from 1.79 GHz to 1.65 GHz as the periodicity increased. Despite these shifts, the peak attenuation remained relatively constant at approximately −27 dB, indicating stable stopband performance across the tested range.

This behavior can be attributed to the reduced mutual electromagnetic coupling between resonators as x increases. Closer resonators exhibit stronger coupling, leading to broader resonance characteristics and increased energy storage within the structure. Conversely, as the spacing widens, coupling weakens, which sharpens the resonance but slightly limits the absorption bandwidth.

The resonance characteristics for each periodicity value are summarized in Table 1. These findings demonstrate that x is an effective design parameter for tuning the resonance frequency and bandwidth of FSS structures, particularly for applications requiring precise frequency selectivity and stable attenuation levels.

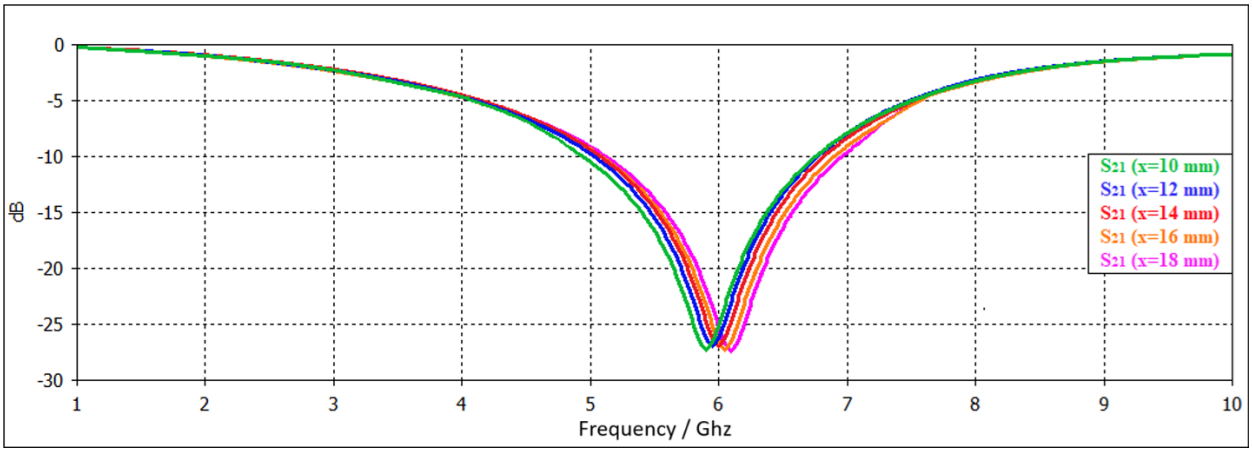

Figure 3. Variation of transmission coefficient (S_{21}) with frequency for different unit cell periodicities

Table 1. Resonance characteristics for varying unit cell periodicity

Unit Cell Periodicity (mm)	Lower Cutoff Frequency (GHz)	Upper Cutoff Frequency (GHz)	Resonance Frequency (GHz)	Bandwidth (GHz)	Maximum Absorption (dB)
10	4.99	6.78	5.89	1.79	−27.13
12	5.02	6.78	5.94	1.76	−27.09
14	5.08	6.81	6.00	1.73	−27.11
16	5.15	6.84	6.06	1.69	−27.08
18	5.20	6.85	6.12	1.65	−27.05

3.2. Effect of outer radius (r) on the S_{21} response

The outer radius (r) of the ring-shaped resonator directly affects the electromagnetic response of the frequency-selective surface (FSS). In this study, r was systematically varied between 5.27 mm and 5.67 mm with increments of 0.10 mm, while the unit cell size (x = 14 mm) and ring width (d = 0.5 mm) were kept constant.

As shown in Figure 4, increasing the outer radius leads to a downward shift of the resonance frequency. The resonance moved from 6.15 GHz for r = 5.27 mm to 5.85 GHz for r = 5.67 mm. Meanwhile, the −10 dB bandwidth exhibited a slight variation, ranging between 1.70 GHz and 1.74 GHz, and the maximum absorption remained stable at approximately −27 dB throughout the range.

This behavior can be explained by the increased current path around the larger ring, which supports resonance at longer wavelengths, thus lowering the resonance frequency. The nearly unchanged maximum absorption suggests that enlarging r does not deteriorate the stopband performance, making it an effective parameter for tuning the resonance without compromising the absorption efficiency.

The detailed resonance characteristics are summarized in Table 2. These results confirm that adjusting r offers a practical method for controlling the operational frequency of the FSS while maintaining consistent absorption performance.

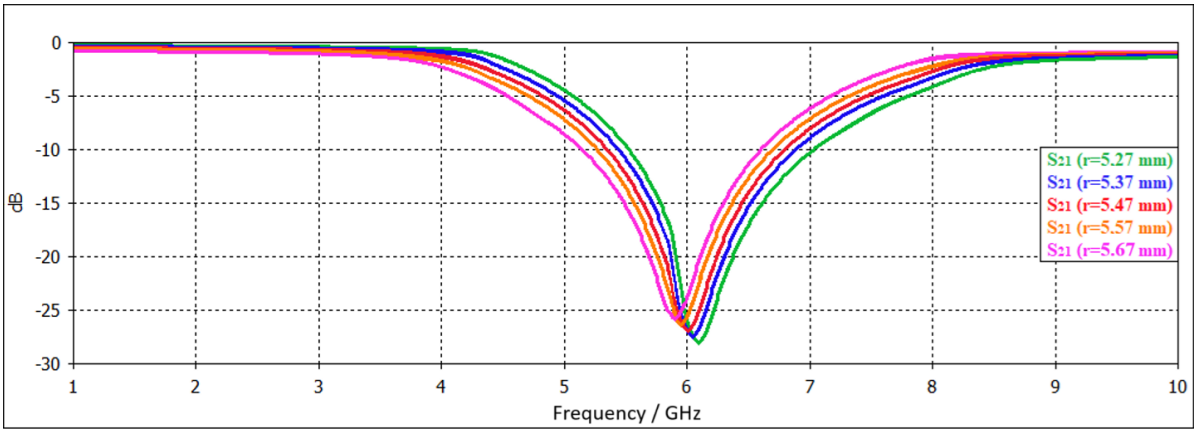

Figure 4. Simulated S_{21} response for varying outer radii

Table 2. Resonance characteristics for varying outer radii

Outer Radius (mm)	Lower Cutoff Frequency (GHz)	Upper Cutoff Frequency (GHz)	Resonance Frequency (GHz)	Bandwidth (GHz)	Maximum Absorption (dB)
5.27	5.34	7.04	6.15	1.70	−27.05
5.37	5.28	7.00	6.06	1.72	−27.09
5.47	5.08	6.81	6.00	1.73	−27.11
5.57	4.95	6.69	5.92	1.74	−27.14
5.67	4.89	6.60	5.85	1.71	−27.10

3.3. Effect of ring width (d) on the S_{21} response

The ring width (d), defined as the difference between the outer and inner radii of the ring-shaped resonator, plays a significant role in shaping the electromagnetic response of the FSS. In this study, d was varied from 0.3 mm to 0.7 mm in 0.1 mm increments, while the unit cell size (x = 14 mm) and outer radius (r = 5.47 mm) were kept constant.

As shown in Figure 5, increasing the ring width d resulted in a progressive downward shift of the resonance frequency. The resonance decreased from 6.15 GHz at d = 0.3 mm to 5.56 GHz at d = 0.7 mm. Additionally, a significant broadening of the absorption bandwidth was observed as d increased.

Moreover, the maximum absorption level remained nearly constant around −27 dB, indicating that increasing the conductive area of the ring does not deteriorate the stopband efficiency. However, excessively large d values may lead to overlapping conductive regions, potentially complicating fabrication and affecting impedance matching.

This trend is attributed to the increased capacitive effect of the resonator with larger ring widths, which lowers the resonance frequency by enhancing the electric field confinement within the structure.

The electromagnetic behavior of the proposed FSS can also be interpreted using an equivalent LC circuit model, where the inductance (L) is associated with the conductive ring path and the capacitance (C) arises from the gaps between adjacent unit cells and the split structure. Variations in geometric parameters such as the outer radius (r), ring width (d), and periodicity (x) modulate the effective inductive and capacitive loading, thereby tuning the resonance frequency. This analogy offers a physical insight into how structural changes affect filtering behavior.

The detailed resonance characteristics are summarized in Table 3. These results demonstrate that d is an effective tuning parameter for adjusting both the resonance frequency and the bandwidth, making it particularly useful for applications that require broad stopband performance.

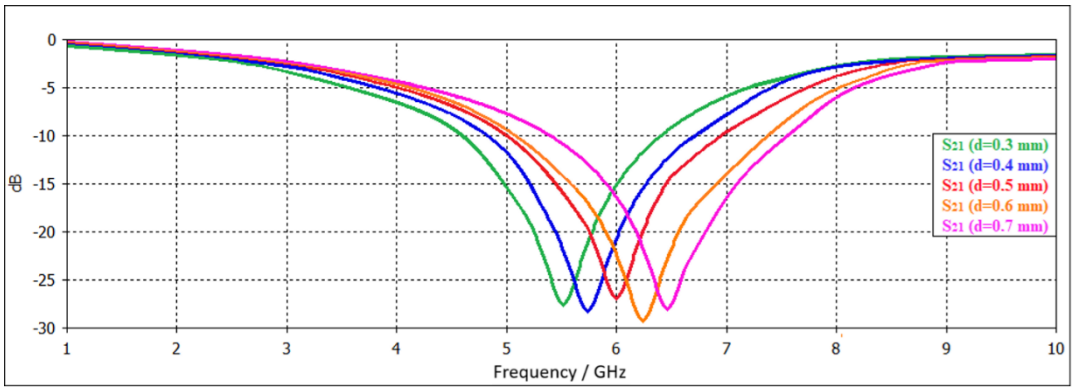

Figure 5. Simulated S_{21} responses for varying ring widths (d)

Table 3. Resonance characteristics extracted from simulations with different d values

Ring Width (mm)	Lower Cutoff Frequency (GHz)	Upper Cutoff Frequency (GHz)	Resonance Frequency (GHz)	Bandwidth (GHz)	Maximum Absorption (dB)
0.30	5.40	6.90	6.15	1.50	−27.12
0.40	5.15	6.84	6.00	1.69	−27.15
0.50	5.08	6.81	6.00	1.73	−27.11
0.60	4.85	6.72	5.75	1.87	−27.10
0.70	4.50	6.65	5.56	2.15	−27.08

3.4. Measured frequency response of the fabricated ring-shaped band-stop FSS

The electromagnetic performance of the fabricated ring-shaped frequency-selective surface (FSS) was evaluated experimentally by measuring its reflection (S_{11}) and transmission (S_{21}) parameters within the 1–10 GHz frequency range. To assess repeatability, three identical FSS samples were fabricated and measured. The resonance frequency deviation was found to be within ±0.06 GHz, indicating high reproducibility. The slight frequency shift (~±0.05 GHz) is attributed to ink spreading during printing, substrate surface roughness, and possible stretching of the textile during curing.

As presented in Figure 6, the FSS exhibits a distinct band-stop filter behavior, characterized by:

- A resonance dip at approximately 6.00 GHz, where the transmission (S_{21}) reaches a minimum of −28 dB.
- A corresponding reflection (S_{11}) peak at around −3 dB, indicating partial reflection of the incident wave.
- High transmission outside the resonance band, confirming the frequency-selective nature of the structure.

At the resonance frequency, the sharp reduction in transmission combined with a moderate reflection implies that a significant portion of the incident electromagnetic energy is attenuated within the structure, rather than being reflected or transmitted. This behavior confirms the band-stop filtering capability of the printed FSS.

The experimental results are consistent with the simulation predictions, validating the design methodology and confirming that the screen-printing process with conductive polyurethane-based paint is a viable fabrication method for flexible electromagnetic devices.

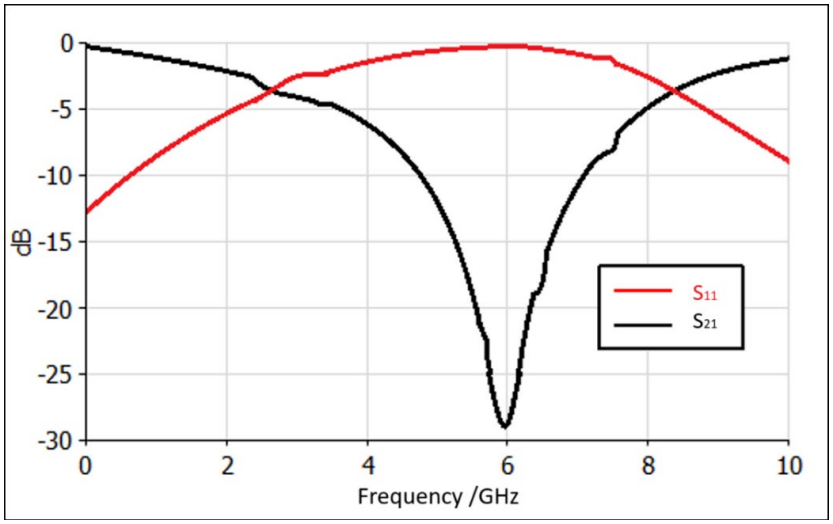

Figure 6. Measured S_{11} and S_{21} responses of the fabricated ring-shaped FSS

The absorption coefficient (A) was calculated using the measured scattering parameters based on the formula:

$$A(f)=1-|S_{11}(f)|^2-|S_{21}(f)|^2$$

where S_{11} and S_{21} represent the reflection and transmission coefficients, respectively. The resulting absorption spectrum is plotted in Figure 7, showing a peak absorption of approximately 50% at the resonance frequency of 6.00 GHz, consistent with the reflection-dominant band-stop behavior rather than a fully absorbing structure.

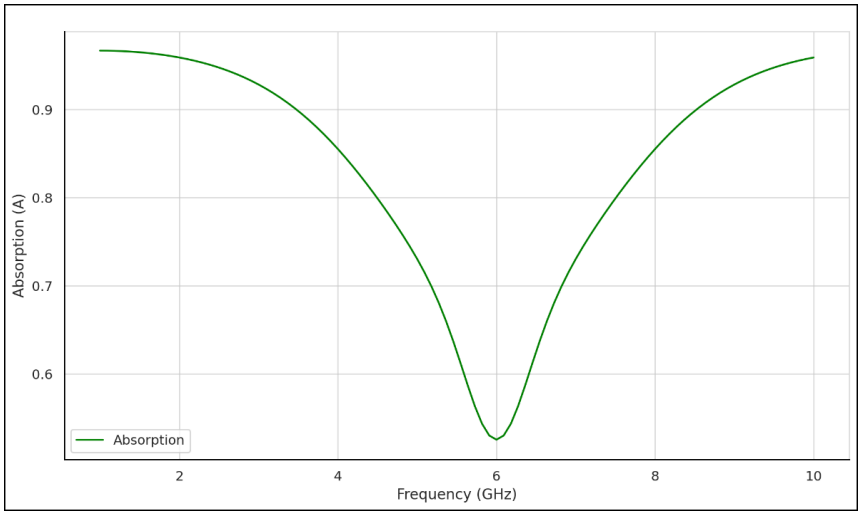

Figure 7. Calculated absorption spectrum of the fabricated ring-shaped FSS based on measured S-parameters

The slight deviation observed between the simulated and measured resonance frequencies can be attributed in part to fabrication tolerances. Variations in ink thickness, screen mesh tension, and curing conditions may influence the electrical properties of the printed pattern, leading to minor discrepancies in the final resonance behavior.

4. Conclusion

In this study, a flexible, ring-shaped frequency-selective surface (FSS) was designed, numerically optimized, screen-printed, and experimentally validated for electromagnetic band-stop applications on textile substrates. The following conclusions can be drawn:

- Parametric analyses confirmed that the geometric parameters—unit cell periodicity (x), outer radius (r), and ring width (d)—strongly influence the resonance frequency and bandwidth characteristics.
- Increasing the unit cell periodicity (x) resulted in a higher resonance frequency due to reduced inter-element coupling.
- Increasing the outer radius (r) shifted the resonance frequency downward while preserving the transmission suppression level, allowing efficient tuning without performance loss.
- Increasing the ring width (d) not only caused a downshift in resonance but also broadened the absorption bandwidth, primarily due to enhanced capacitive coupling.
- The screen-printed FSS structure on a 150 mm × 150 mm textile surface exhibited excellent agreement between simulation and measurement, confirming the reproducibility of the proposed fabrication process.

The experimentally measured resonance occurred at approximately 6.00 GHz, consistent with the simulation results. The transmission suppression reached −28 dB, and the absorption peak, calculated from measured S-parameters, reached approximately 50%, indicating partial absorption behavior. This confirms that while the structure effectively blocks electromagnetic transmission, a considerable portion of the energy is reflected rather than fully absorbed.

Overall, the proposed design demonstrates the feasibility of developing low-cost, flexible, and high-performance metamaterial-based FSS structures using scalable screen-printing techniques. Compared to existing textile-based FSS implementations, the use of custom-formulated PU-based conductive ink, combined with validated mechanical-electromagnetic compatibility, offers a unique contribution. This structure holds strong potential for wearable shielding systems, stealth garments, and conformal electromagnetic devices. Given its lightweight and flexible nature, the developed FSS can be integrated into smart garments for wireless signal management, wearable EMI shielding, or military textiles for stealth and camouflage applications.

Future studies will focus on exploring tunable or reconfigurable geometries, evaluating long-term durability under repeated deformation, and enhancing absorption performance through multi-layered or hybrid material strategies.

Declaration of Conflict of Interests

The authors declare that there is no conflict of interest. They have no known competing financial interests or personal relationships that could have appeared to influence the work reported in this paper.

References

[1.] Pendry, J.B., Calculating photonic band structure. Journal of Physics: Condensed Matter, 8 (1996) 1085.

[2.] Pendry, J.B., Negative refraction makes a perfect lens. Physical Review Letters, 85 (2000) 3966-3969.

[3.] Pendry, J.B., Holden, A.J., Robbins, D.J. and Stewart, W.J., Low frequency plasmons in thin-wire structures. Journal of Physics: Condensed Matter, 10 (1998) 4785.

[4.] Pendry, J.B., Holden, A.J., Robbins, D.J. and Stewart, W.J., Magnetism from conductors and enhanced nonlinear phenomena. IEEE Transactions on Microwave Theory and Techniques, 47 (1999) 2075-2084.

[5.] Pendry, J.B., Holden, A.J., Stewart, W.J. and Youngs, I., Extremely low frequency plasmons in metallic mesostructures. Physical Review Letters, 76 (1996) 4773-4776.

[6.] Shelby, R.A., Smith, D.R. and Schultz, S., Experimental verification of a negative index of refraction. Science, 292 (2001) 77-79.

[7.] Viktor, G.V., The electrodynamics of substances with simultaneously negative values of ε and μ. Soviet Physics Uspekhi, 10 (1968) 509.

[8.] Vinoy, K.J. and Jha, R.M., Trends in radar absorbing materials technology. Sadhana, 20 (1995) 815-850.

[9.] Wakatsuchi, H., Sievenpiper, D.F. and Christopoulos, C., Designing flexible and versatile metamaterial absorbers. IEEE Electromagnetic Compatibility Magazine, 5 (2016) 76-82.

[10.] Wang, B., Koschny, T. and Soukoulis, C.M., Wide-angle and polarization-independent chiral metamaterial absorber. Physical Review B, 80 (2009) 033108.

[11.] Wang, B., Zhou, J., Koschny, T. and Soukoulis, C.M., Nonplanar chiral metamaterials with negative index. Applied Physics Letters, 94 (2009) 151112.

[12.] Watts, C.M., Liu, X. and Padilla, W.J., Metamaterial electromagnetic wave absorbers. Advanced Materials, 24 (2012) OP98-OP120.

[13.] Withayachumnankul, W., Jaruwongrungsee, K., Tuantranont, A., Fumeaux, C. and Abbott, D., Metamaterial-based microfluidic sensor for dielectric characterization. Sensors and Actuators A: Physical, 189 (2013) 233-237.

[14.] Wright, R., Broadband microwave energy absorptive structure. Google Patents, (1974).

[15.] Wu, T.K., John, W., and Sons, Frequency selective surface and grid array. A Wiley-Interscience Publication, (1995).

[16.] Xin, W., Binzhen, Z., Wanjun, W., Junlin, W. and Junping, D., Design, fabrication, and characterization of a flexible dual-band metamaterial absorber. IEEE Photonics Journal, 9 (2017) 1-12.

[17.] Zhang, S., Park, Y.-S., Li, J., Lu, X., Zhang, W. and Zhang, X., Negative refractive index in chiral metamaterials. Physical Review Letters, 102 (2009), 023901.

[18.] Zhao, R., Koschny, T. and Soukoulis, C.M., Chiral metamaterials: Retrieval of the effective parameters with and without substrate. Optics Express, 18 (2010), 14553-14567.

[19.] Zhao, R., Zhang, L., Zhou, J., Koschny, T. and Soukoulis, C.M., Conjugated gammadion chiral metamaterial with uniaxial optical activity and negative refractive index. Physical Review B, 83 (2011) 035105.

[20.] Zheludev, N.I., The road ahead for metamaterials. Science, 328 (2010) 582-583.

[21.] Zheludev, N.I., Applied physics. Obtaining optical properties on demand. Science, 348 (2015), 973-974.

[22.] Zhu, B., Wang, Z.B., Huang, C., Feng, Y., Zhao, J. and Jiang, T., Polarization insensitive metamaterial absorber with wide incident angle. Progress in Electromagnetics Research, 101 (2010) 231-239.

[23.] Yang, Y., Song, C., Pei, R., Wang, J., Liu, Z., Zhang, Y., & Shen, J., Design, characterization and fabrication of a flexible broadband metamaterial absorber based on textile. Additive Manufacturing, 69 (2023) 103537.

[24.] Choi, J., Daecheon, L., and Sungjoon L., Screen-Printed metamaterial absorber using fractal metal mesh for optical transparency and flexibility. Fractal and Fractional 8 (2024) 284.

How to Cite This Article

Kiziltas, H. and Ozturk, G., Design, Parametric Analysis, and Experimental Validation of a Screen-Printed Flexible Band-Stop Frequency Selective Surface, Brilliant Engineering, 3(2025), 41040.
https://doi.org/10.36937/ben.2025.41040